Available online at www.sciencedirect.com
SCIENCE DIRECT
Neural Networks 18 (2005) 123–144
Neural Networks
www.elsevier.com/locate/neunet

Chaotic dynamics of a behavior-based miniature mobile robot: effects of environment and control structure

Md. Monirul Islam[a], K. Murase[b,*]

[a]Department of Computer Science and Engineering, Bangladesh University of Engineering and Technology (BUET), Dhaka 1000, Bangladesh
[b]Department of Human and Artificial Intelligence Systems (HART), University of Fukui, 3-9-1 Bunkyo, Fukui 910-8507, Japan

Received 9 January 2002; revised 14 September 2004; accepted 14 September 2004

Abstract

To study the regularity and complexity of autonomous behavior, the flow of sensory information obtained in autonomous mobile robots under various conditions was analyzed as a complex system. Sensory information time series X_n was collected from a miniature mobile robot during free navigation, and plotted on the return map, the graph of $X_{n+\tau}$ vs. X_n. The plot exhibited a characteristic trajectory, representing the regularity of the time series. Correlation integral and Lyapunov exponent analysis also showed properties of deterministic chaos; the presence of fractal dimension and positive Lyapunov exponent. Analysis of sensory information obtained in the robot with three different neural controllers revealed that the autonomous robot behaves in such a way that the flow of sensory information is governed by a deterministic rule, and this pattern is unique to each controller. Furthermore, the analysis in various environments exhibited that transitions from one trajectory to another on the return map occur during the course of autonomous behavior. The fractal and Lyapunov dimensions calculated in various conditions indicate that these dimension could be utilized to quantify the complexity of autonomous behavior and the relative difficulty of tasks. Analyses at different evolutionary stage revealed that behavioral performance correlates with fractal dimension. These studies using a miniature mobile robot that allowed to idealize the experimental conditions demonstrated firmly that the complex analysis could be utilized in evaluation and optimization of autonomous systems and the behavior.

Keywords: Chaos; Behavior-based robot; Mobile robot; Performance measure of robot; Self-organization

1. Introduction

The sensory information perceived by an autonomous robot, as well as by living creatures, reflects dynamic interactions between the robot and the environment in which the robot is situated (Biro & Ziemke, 1998; Brooks, 1991; Degn, Holden, & Olsen, 1997; Pfeiffer, 1995, Pfeiffer & Scheier, 1997). Even in a static environment, the sensory information received through sensory organs is dynamic because of the behavior of the robot itself. In the behavior-based robotics (Brooks, 1986, 1991), motor control signals are generated by the flow of sensory information, which is a function of the robot's own behavior. Therefore, during autonomous behavior, which is goal-directed and/or self-organized, the sensory information flow should have an organization, or a hidden regularity (Odagiri, Monirul Islam, Okura, Asai, & Murase, 1999; Odagiri, Wei, Asai, & Murase, 1998a; Odagiri, Wei, Asai, Yamakawa, & Murase, 1998b; Ziemke, 1996a,b). That is, although fluctuation in the time series of sensory signals looks as if random, there should exist a hidden regularity underlying it. Although, the internal representation generating organized behavior of the autonomous robot has been the target of intensive research (e.g. Pfeiffer, 1995; Pfeiffer & Scheier, 1997) and the robot's internal states have been investigated (e.g. Ziemke, 1996a,b, 1998), further understanding of the hidden regularity in their behavior as well as that of internal states is needed.

The phenomenon that appears random but is regulated under a deterministic rule is called deterministic chaos, and its nature can be analyzed mathematically (Holden, 1986; Jackson, 1989; Parker & Chua, 1987). Chaos has been found

* Corresponding author. Tel.: +81 776 27 8774; fax: +81 776 27 8420.
E-mail address: murase@synapse.his.fukui-u.ac.jp (K. Murase).

0893-6080/$ - see front matter © 2004 Elsevier Ltd. All rights reserved.
doi:10.1016/j.neunet.2004.09.002

in living organs such as in brain activity (Babloyantz, Salazar, & Nicolis, 1985; Babloyantz & Destexhe, 1986), neurons (Hayashi, Ishizuka, & Nicolis; 1985) and axons (Matsumoto, Aihara, Hanyu, Takahashi, Yoshizawa, & Nagumo, 1987), as well as artificial neural networks (Aihara, Aihara, Takabe, & Toyota, 1990; Ikeguchi, Aihara, Ito, & Utsunomiya, 1990) and others (Degn et al., 1997; Ott, 1993). In the brain, spontaneous neuronal activity exhibits some properties of deterministic chaos, and an alteration in its profile occurs when a change in sensory information takes place (Degn et al., 1997; Freeman, 1991, 1994a). It has been thus considered that this chaos and transition might be the underlying concept of perception and goal-directed, organized behavior (Freeman, 1994b; Kay, Lancaster, & Freeman, 1996).

The regularity in the sensory information during autonomous behavior is also found in artificial life. In an autonomous mobile robot, the time series of sensory data obtained during free navigation exhibits regularity on a phase-plane plot called the return map (Smithers, 1995). It has a fractal dimension of non-integer value, an important property of deterministic chaos (Holden, 1986; Lorenz, 1994; Ott, 1993; Parker, & Chua, 1987). It is even suggested that the regularity could be used as a performance measure of autonomous robots. However, it is yet to be shown how the regularity of a robot is altered when its environment changes, and how it differs among robots with various controllers. In such analysis, it is necessary to collect sensory data sets of long period during free navigation of robots in various conditions and it has been difficult to perform the reliable experiments.

The purpose of this study is thus two folds. Firstly, we intended to reveal whether or not phenomena similar to that which takes place in the brain also takes place in artificial life. We used a miniature autonomous mobile robot suitable for rigorous, reproducible experiments. We obtained results showing that the time series of sensory information obtained during free navigation exhibits regularity, and that it has the nature of deterministic chaos. We also investigated whether or not the regularity changes in accordance with the environmental alterations.

Secondly, we tried to reveal how the regularity differs among individuals. This is essential for understanding the nature of autonomy, as well as for testing whether or not it can be utilized in practice as a performance measure of autonomous robots. A given task could be difficult for a particular robot but not for the others depending upon their control scheme, and the quantification of the hardness is highly desirable. We thus investigated how the regularity varies when various neural controllers were loaded in the robot and compared the regularity and performance among them.

This paper consists of five sections. In Section 2, we describe the robot we used, and the way we collected and constructed sensory information. In Section 3, methods and results of analysis with the return map, the correlation integral, Lyapunov exponent and the relation with behavioral performance we used are described. In Section 4, we discuss the analyzed data in terms of individual differences of regularity, the effect of environment on regularity, transition of autonomous behavior, and the fractal dimensions. Section 5 is Summary and Conclusion.

2. Experiments

This section describes the three types of autonomous mobile robots used in this study, and the collection of the sensory information during free movement in four different environments. Three types of robots were modeled by three different controllers loaded in a miniature mobile robot. In order to perform reliable analysis, it is necessary to obtain sensory time series of long duration with minimal noise. We therefore, utilized a miniature mobile robot. It allowed long-term recordings on a desk-top environment where external noise could be maintained minimal. The robot was designed as simple as possible, just sufficient to perform the desired task. We used a simple neural network as a controller with the minimal number of sensors, so that the results of analysis became clear enough to exhibit the essence of findings. Genetic evolution was used to determine the parameters of the robot controllers so that the robot was optimized for a given environment. Sensory information time series were collected in four environments including the evolved one for the analysis described in Section 3.

2.1. Experiments with three types of autonomous mobile robots

Three types of robots were constructed by loading different neural networks into a miniature mobile robot. The neural network was intended to produce motor control signals based on the proximity sensor signals. The connection weights of each neural network were determined by the genetic evolution for navigation and obstacle avoidance in a field called the Maze environment.

2.1.1. Miniature mobile robot

We used a real mobile robot Khepera, whose structure and function have been well described elsewhere (Mondada, Franzi, & Ienne 1993). In short, its size is small: 55 cm in diameter, 30 mm in height, and 70 g in weight. It consists of two boards: the CPU board and the sensory-motor board. The CPU board contains a microprocessor (Motorola MC68311) with 128 Kbytes of EEPROM and 256 Kbytes of static RAM, an A/D converter for the acquisition of analogue signals coming from the sensory-motor board, a proportional-integral–differential (PID) controller for the motor control, and a RS232C serial port together with power-supply terminals which is used for data transmission to and from an external computer system and for providing electricity from an external power-supply unit. The microprocessor can execute programs downloaded

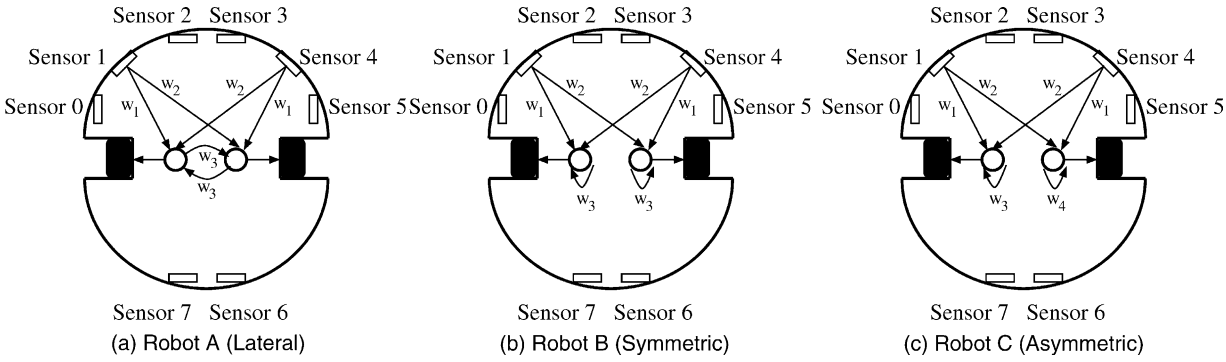

Fig. 1. Three types of autonomous mobile robots.

from the external workstation. In addition, multiple processes can be executed in parallel by time-sharing on the on-board microprocessor.

The motor system uses two lateral wheels and supporting pivots in front and back. Each wheel is controlled by a DC motor and is equipped with an incremental encoder. The motor can rotate in both directions by the output from the CPU to the PID controller. There are eight infrared (IR) proximity sensors: six on the front side and two on the back (see Fig. 1). These sensors can detect objects within 3 cm or so by emitting infrared light and measuring its reflection. The values can be utilized by the microprocessor through the A/D converter for such functions as generating motor control signals and analyzing the scenery perceived by the robot.

The use of this type of miniature robot was suitable for this study. Evolutionary processes and data collection are quite time consuming in general. The desk-top set-up allowed us trials and errors in experiment without significant changes in the environments and in the mechanics of the robot throughout the duration of experiment.

2.1.2. Experimental set-up

As shown in Fig. 2, an aerial cable from the RS232C port of the robot was attached to a serial port of a UNIX

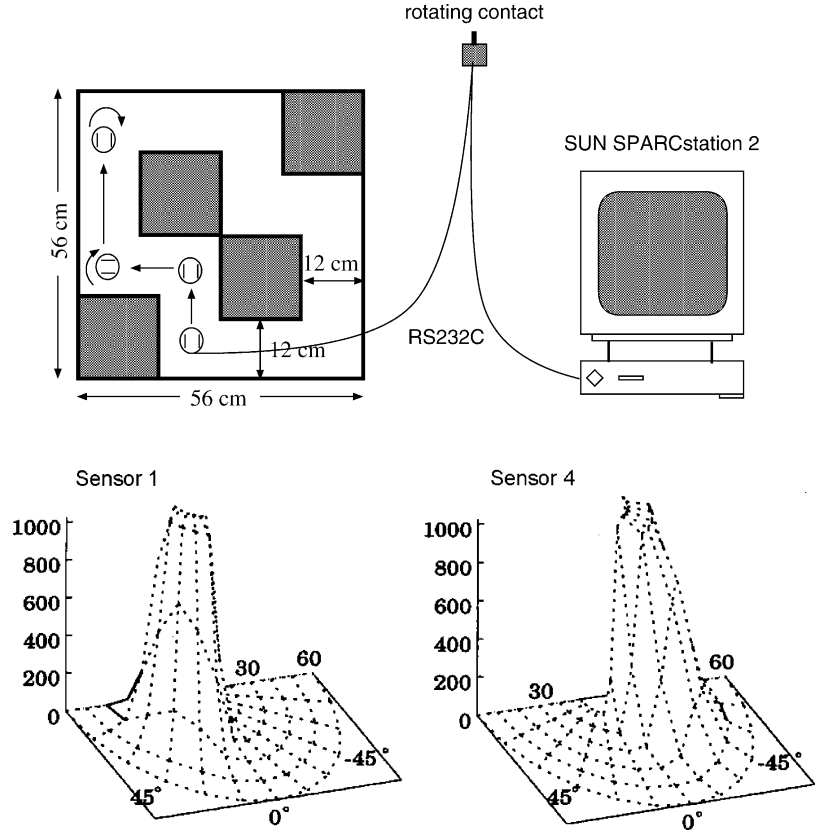

Fig. 2. Experimental set-up, the evolved environment, and the directional sensitivity of the sensors.

workstation SUN SPARCstation 2 via a miniature rotating contact. The generation of autonomous behavior by calculating motor outputs from sensor readings, and monitoring and storing sensor, motor and encoder values were performed by the on-board microprocessor and memory, while other processes such as constructing neural networks, executing genetic operations, and detailed analysis of sensory signals were managed by the external workstation.

2.1.3. Three types of robots

Fig. 1 shows the three types of two-layered neural networks loaded on the on-board microprocessor to produce motor control signals from sensor signals. These robots with different neural networks were designated as robots A, B, and C. The neural networks of robots A, B, and C were characterized by the presence of lateral connections, symmetric recurrent connections, and asymmetric recurrent connections, respectively. The connection weights were symmetric except for the asymmetric recurrent connection of robot C. There existed, so to speak, a structural difference of the network between robot B and C, and a topological difference in robot C to robots A and B.

Unlike most of the previous works regarding obstacle avoidance (e.g. Floreano & Mondada, 1994, 1996; Naito, Odagiri, Matsunaga, Tanifuji, & Murase, 1997; Nolfi, Floreano, Miglino, & Mondada, 1994), the input signals coming from only two front sensors, 1 and 4, were fed to the neural network. It has been reported that two front sensors are sufficient for navigation in simple environments such as that shown in Fig. 2, and the use of two sensors simplifies the following analysis of the sensory information as well (Odagiri et al., 1998a,b). The sights of both sensors illustrated are in Fig. 2. The robot was placed at the center of circles, and the sensor readings were measured when a white paper wall was placed at various positions against the robot. The sensor could detect the wall within 60 mm from the center of the robot or 37.5 mm away from each sensor. Since the sensor value increased sharply from near zero to near maximum for the wall at 30–20 mm from the sensor, a several mm change in the distance within this range could produce a large change in the sensor value on an order of several hundred. Each sensor covered approximately 90 degrees of the field, and thus by using both sensors 1 and 4, the wall located in the entire front area of the robot could be detected.

Each output of the neural network was produced as a weighted sum of two sensor signals and one lateral or recurrent input as follows

$$S_p = S_b + G\sum w_i x_i \tag{1}$$

where S_p, S_b, G, w_i, and x_i represent the output for the motor, the base navigation speed of the motor, the global gain, the connection weights from sensors and output cell, and the signals from corresponding sensors and output cell, respectively. The values for S_b and G were set to 5 cm/s and 1/800, respectively.

2.1.4. Genetic evolution

For each of the robots, A, B, and C, a simple genetic algorithm (Holland, 1975) was used to determine the values of connection weights in the neural network The robots were evolved in the field called the Maze environment shown in Fig. 2. Each individual in a population had the same constant length of chromosome corresponding to the number of connections in the neural network. Each weight was encoded on a gene of five bits. The first bit determined the sign of the weight and the remaining four bits its strength. The length of a chromosome thus became 15 bits in robots A and B, and 20 bits in robot C.

Each chromosome corresponding to an individual in a population was generated by the external workstation, and loaded down to the on-board microprocessor. After decoding into the corresponding neural network, the robot was allowed to move in the environment shown in Fig. 2 with the neural network's input and output values as well as encoder values sampled every 0.1 s. These values were then uploaded to the workstation for fitness evaluation. Between individuals, the robot changed its position randomly by Braitenberg algorithm (Braitenberg, 1984) in order to avoid the effect of the previous individual's action. This procedure was repeated for all individuals. When all individuals had been tested, three genetic operators-selective reproduction, crossover, and mutation-were applied to create a completely new population of the same size. The fitness function F used to evaluate each individual in a population was expressed as follows

$$F = D(1 - v)(1 - s) \tag{2}$$

Here D, v, and s were the normalized values of the total mileage of both motors, the difference mileage between the two motors, and the total of two sensor values, respectively, which were acquired every 0.1 s for an individual life-time period of 5 s. The fitness function has been a standard for developing the obstacle-avoidance and navigation capability (e.g. Floreano & Mondada, 1994, 1996; Nolfi et al., 1994). One population of 10 individuals was evolved for 50 generations of each robot. The cross-over rate, the mutation rate, and the elite preservation rate in the roulette selection used in the genetic operation were 0.7, 0.02, and 0.5, respectively.

Fig. 3 shows examples of the evolution processes for robots A, B, and C. Some individuals who faced against walls with slipping wheels got high scores at the initial stage of evolution, but the behavior improved steadily after generations. Due to the short length of chromosomes, the robots learned to navigate and avoid obstacles very quickly, often within 30 generations. The best individuals in generations 35–50, having fitness scores of 0.12–0.2, could navigate the whole environment very smoothly.

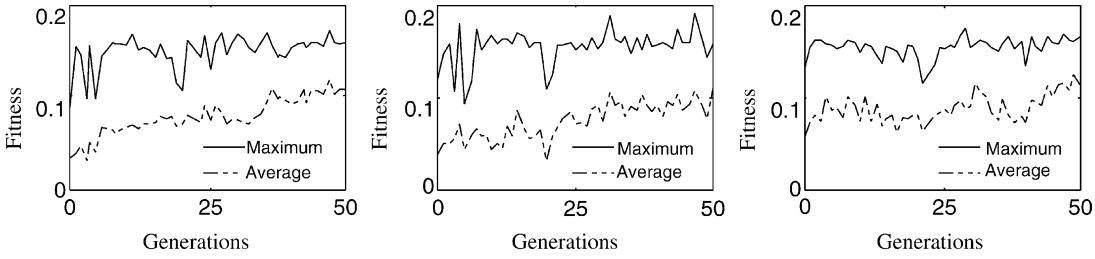

Fig. 3. Evolution processes of three robots.

They never bumped into walls and corners, and rather maintained a straight trajectory when possible. Connection weights of the best individuals were as follows: For Robot A, $w_1 = +8$, $w_2 = -14$, and $w_3 = +9$. For Robot B $w_1 = +4$, $w_2 = -12$, and $w_3 = +11$. For robot C, $w_1 = +4$, $w_2 = -16$, $w_3 = +5$, and $w_4 = +12$. We used these best individuals throughout the following studies.

Through visual observation of behavior, distinguishing the three robots from each other was very difficult. This was evidenced by the sensory information obtained in the Maze environment as shown in Fig. 4. Sensory signals exhibited periodical peaks in a similar manner in all three robots, but the magnitudes varied among them. This indicates that all of them rotated in the path of the field very well, but the distance from the walls, especially at the corners, varied among them by several millimeters.

2.2. Sensory information in four different environments

Each of the best robots A, B, and C obtained by genetic evolution was placed in four different fields called the Maze, Square, Dynamic, and the Straight-Corridor environments. During free navigation in each environment, the proximity sensor values of a robot were continuously sampled. Using the sampled sensory signal, a time series representing the proximity of the robot to the front obstacle, which we call sensory information, was constructed. For each robot, four time series, each for one environment, were constructed. Thus, a total of twelve time series were constructed for three robots in this study.

2.2.1. Environments

The four environments in which sensory information was collected are shown in Fig. 5. White non-glossy card board was pasted on straight wooden bars and they were used to make the walls of the path and obstacles in the field. The Maze environment was identical to the one wherein robots evolved. Notice that the Maze environment consisted of straight paths and right-angled corners. The Square environment also consisted of straight paths of the same width and right-angled corners as those of the Maze environment, but contained only one-directional turns. In the Dynamic environment, an obstacle was placed manually at 6–8 cm in front of the robot navigating. The robot had to turn to avoid a head-on collision, and after turning the robot again faced another obstacle in front placed manually. This was repeated during its entire life. The Straight-Corridor environment had the same width as the straight paths of the Maze and Square environments. The robot was placed in the field to go along the path, but not to face the wall. The path was sufficiently long to allow the sensory information to be collected for approximately 20 s because the robot's navigation speed was about 5 cm/s.

In order to avoid environmental noise, a number of precautions were taken in this study. Experiments were done

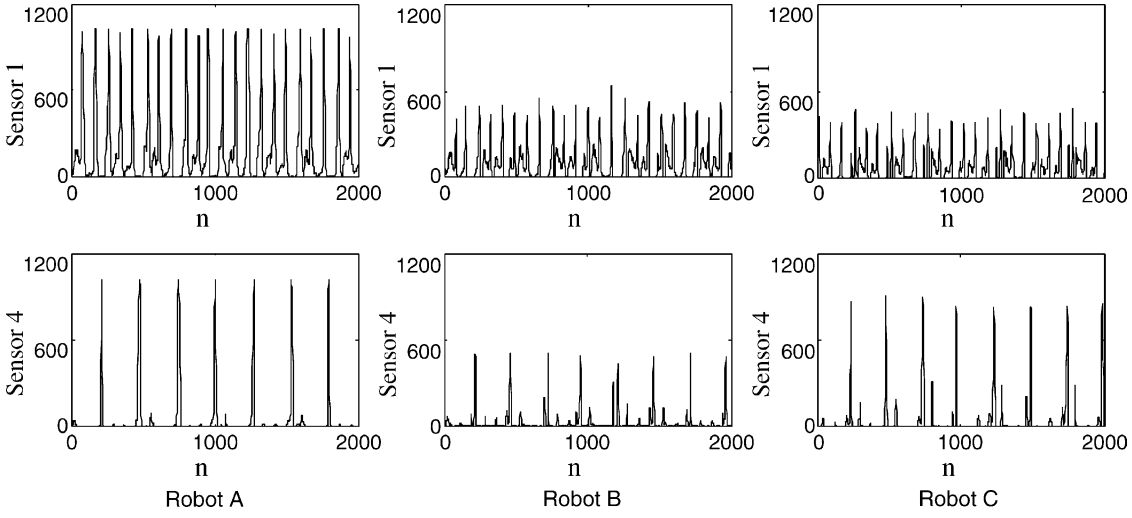

Fig. 4. Examples of signals detected by sensors 1 and 4.

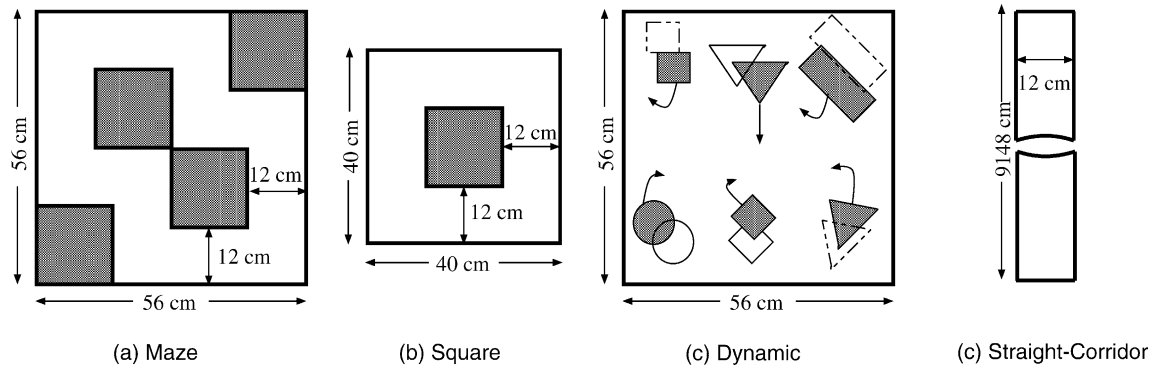

Fig. 5. Tested environments.

in complete darkness. Records of sensor signals were taken mostly in the late night in order to avoid unexpected exposure of light during the course of recording. As apparent from Fig. 2, the proximity sensors generated output signals when the obstacles were within 3 cm or so. Any obstacles away from it, or any movements occurred far from it were unlikely to produce any signal. Therefore, the output of the sensors contained only the information from walls and/or obstacles within c.a. 3 cm with minimal noise from environment.

2.2.2. Proximity of the robot to the front obstacle

For each robot, the values of sensors 1 and 4 were continuously sampled every 0.1 for 3072 s during free navigation in the Square, Maze, and Dynamic environments, and Straight-Corridor environment. Since the size of on-board memory of the robot was limited, it was not possible to take 30720 (i.e. 3072/0.1) points of data continuously. Therefore, we made intermissions during the course of recording and transmitted the data to the host computer during the period.

In this study, robots moved for a period collecting 512 points of data, and stopped until the transmission of the collected data was completed. And then robots again started moving from the position. This was repeated until 30720 points of data were collected for all environments. Since data was sampled at every 0.1 sec, collecting 512 points took 51.2 s. During the period, robots could moved a considerable portion of the path in the environment. For example, the entire path of the Maze and Square environments could be gone through since the navigation speed of robots was about 5 cm/s and the size of the environments was 54 cm square. No human intervention was introduced during the course of data collection. Thus the data was continuous, although the navigation was intermittent.

Since the robot was stopped during the transmission of data, the problem of inertia might take place when stopping or starting its movement. We therefore performed a set of preliminary experiments with various speeds (5, 10, 20 cm/s) of robots to see whether any discontinuity of the sensory values took place. At the speed of 20 cm/s there observed an discontinuity in the sensor values due to slipping. However, no such phenomena was observed at slower speeds. Therefore, we concluded that a quasi-steady state could be achieved when the navigation speed was less than 10 cm/s. However, as mentioned previously, actual speeds of robots after evolution were far slower, about 5 cm/s. We thus assured that the experiments were free from the problem of inertia.

Portions of the time series obtained from sensors 1 and 4 in Maze environment are illustrated in Fig. 4. As mentioned previously, the signals in three robots were nearly cyclic and the periods were almost identical among the robots. This indicates that all three robots navigated well along the path of the field in a manner similar to each other. Fig. 6 illustrates the relations between signals from sensor 1 and 4 obtained in Robot A. It is apparent from this figure that, although the robot looked as if it was symmetrically made, there exists delicate differences between left and right sides of sensors, motors, locations of parts, electrical circuit properties, and so on, resulting an asymmetry in the sensory signals. This representation of sensory signals was thus too sensitive to the residual asymmetry of the robot itself. And also, although the robot indeed generated organized behavior (i.e. avoiding obstacles to navigate), it was difficult to perceive the organization in this form of plots, especially in those obtained in Dynamic environment. We then tried to find another measure that clearly described the dynamics of the data as follows:

The values from sensors 1 and 4 could be analyzed as a two dimensional time series. For mobile robot whose task is to avoid obstacles and navigate, however, one of the most essential information is the time series of the distance to front object. Since left front sensor we used covered nearly left half of the robot's front sight, and right sensor covered another half, the root square of both sensor values represents well this information. By focusing on this particular information, we intended to avoid mixing up with other information, such as the relation between left and right, which would behave like noise when the length of time series is limited. Thus, the two-dimensional sensory-signal time series consisted of values from sensors 1 and 4 were

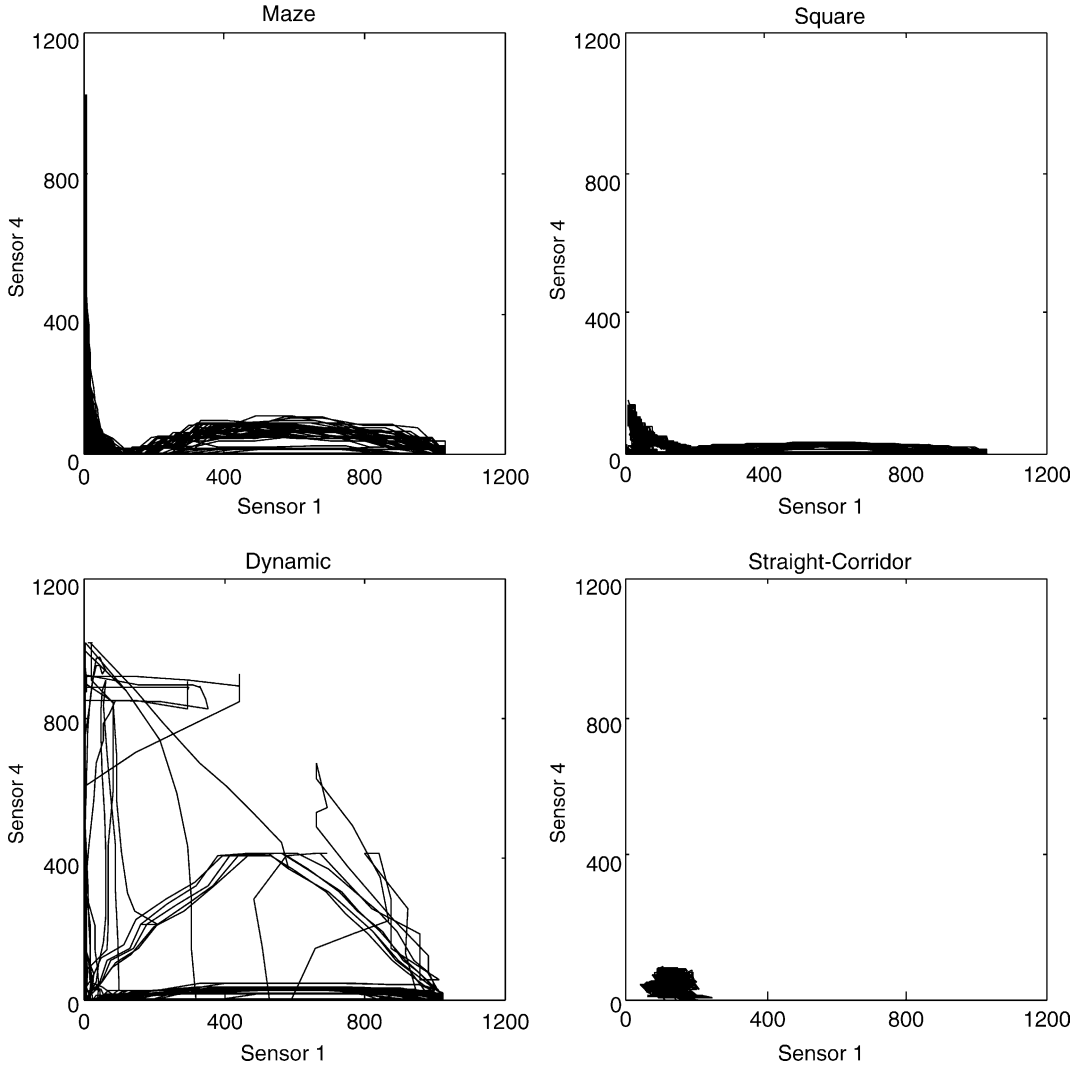

Fig. 6. Two-dimensional plots of sensor signals.

reduced down to one-dimensional sensory information by calculating the root square as follows

$$X_n = \sqrt{S_1(n)^2 + S_4(n)^2} \quad n = 1, 2, \ldots \tag{3}$$

where $S_1(n)$ and $S_4(n)$, $n=1, 2,\ldots$, are the time series from sensors 1 and 4, respectively. Although the smooth behavior of time series indicates that the amount of observational noise is small (Fig. 4), we calculated X_n as real values by filtering the root square of two sensors value with a 7-point moving average (MA) filter. It has been known that a MA filter with an adequate time span does not change the structure of the attractor in the time series (Sauer, Yorke, Casdagli, & Embedology, 1991). In order to find the appropriate time span, we did several trials with various time spans. We found that the return map with a particular time span, in our study it was 7, was very much similar with the return map without it. We took that time span for filtering.

Original quantum error of each sensor value is approximately $1/(2\times1023)\cong5\times10^{-4}$ of the maximum value of 1023 since an analogue-to-digital converter of 10 bits was used. Therefore, the actual error associated with the analogue to digital conversion should be less than, for example, $5\times10^{-4}/\sqrt{2\times7}$ ($\equiv-78$ db) of the maximum value.

In this study, we call the time series X_n the sensory information. Parts of the sensory information were illustrated in Fig. 7. It is apparent that all the robots navigated well in the Maze and Square environments as evidenced by the periodical peaks. As well, in the Dynamic environment, all robots responded well to the obstacle by reflective movements. In the Straight-Corridor environment, each of the robots maintained themselves at the center of the path or along a side wall during navigation, as apparent in Fig. 7.

3. Analysis

Twelve sets of the sensory information, obtained in four different environments by three robots, were analyzed by plotting them on the return map, and calculating

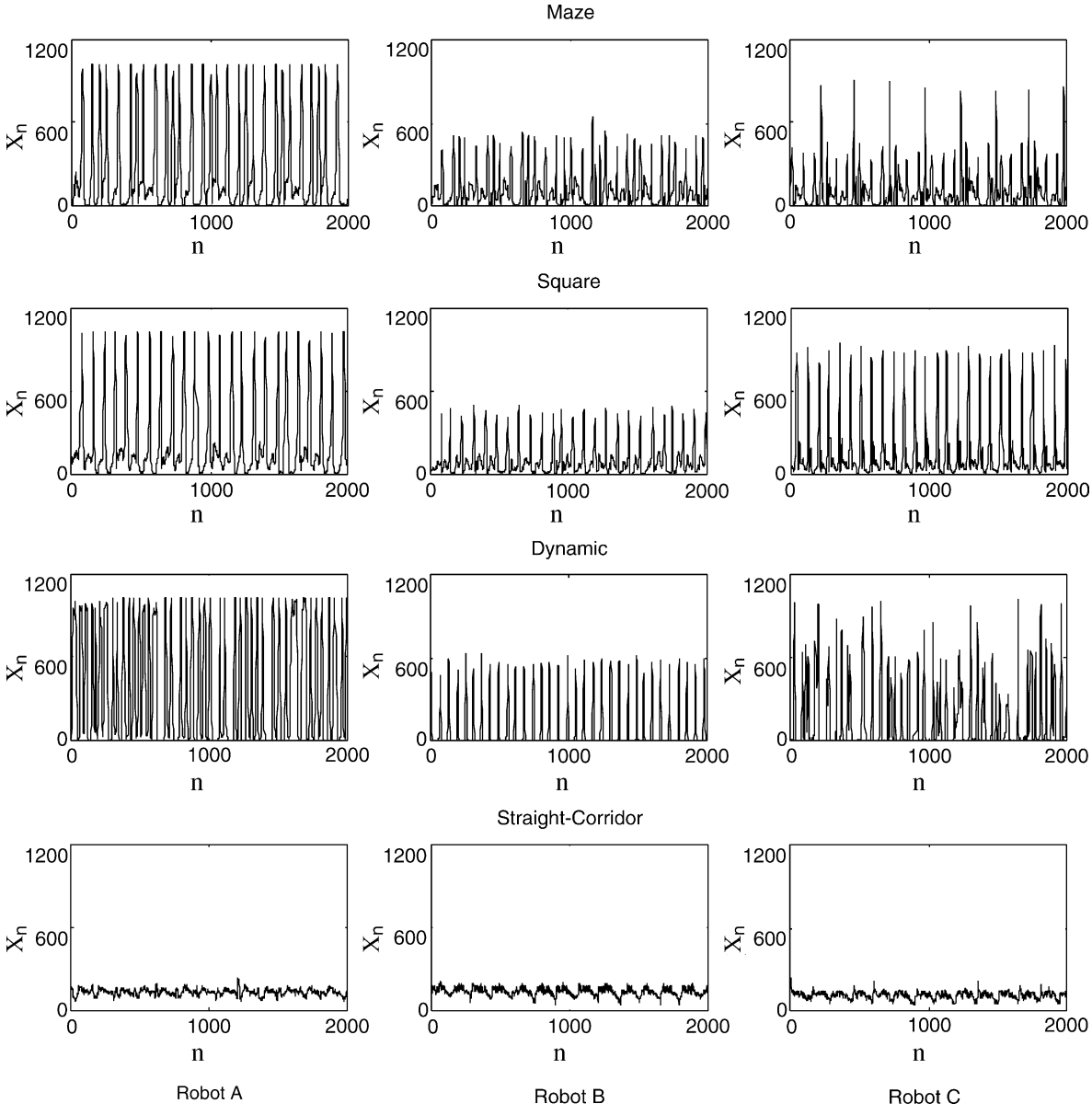

Fig. 7. Sensory information of three robots in four different environments.

the correlation integrals and Lyapunov exponents Each sensory information exhibited a characteristic trajectory on the phase plane, indicating the presence of hidden regularity in the time series. One of the most important characteristics of the deterministic chaos in a time series is the presence of the fractal dimension (Holden, 1986; Jackson, 1989; Lorenz, 1994; Ott, 1993). We estimated this by means of correlation integral analysis.

3.1. Regularity on return map

Embedding the time series is one of the methods to reconstruct the hidden background dynamics (Takens, 1981) The m-dimensional phase space Y_n is constructed from the observed one-dimensional time series X_n as follows:

$$Y_n = (X_n, X_{n+\tau}, \ldots, Xn + (m-1)\tau) \quad (4)$$

where the parameter τ is known as the delay parameter. If the time series X_n is a part of the system variables which obeys some deterministic dynamics, the embedded trajectory Y_n in the reconstructed phase space represents the structure of such dynamics (Yamaguchi, Watanabe, Mikami, & Wada, 1999). The 2-dimensional phase space plot $X_{n+\tau}$ vs. X_n, known as the return map, has been widely used to reveal the dynamics of time series (Aihara et al., 1990; Degn et al., 1997; Freeman, 1991; Hayashi et al., 1985; Holden, 1986; Ikeguchi et al., 1990).

The return maps for robots A, B, and C in the Maze environment, and the return maps for robot A in other three

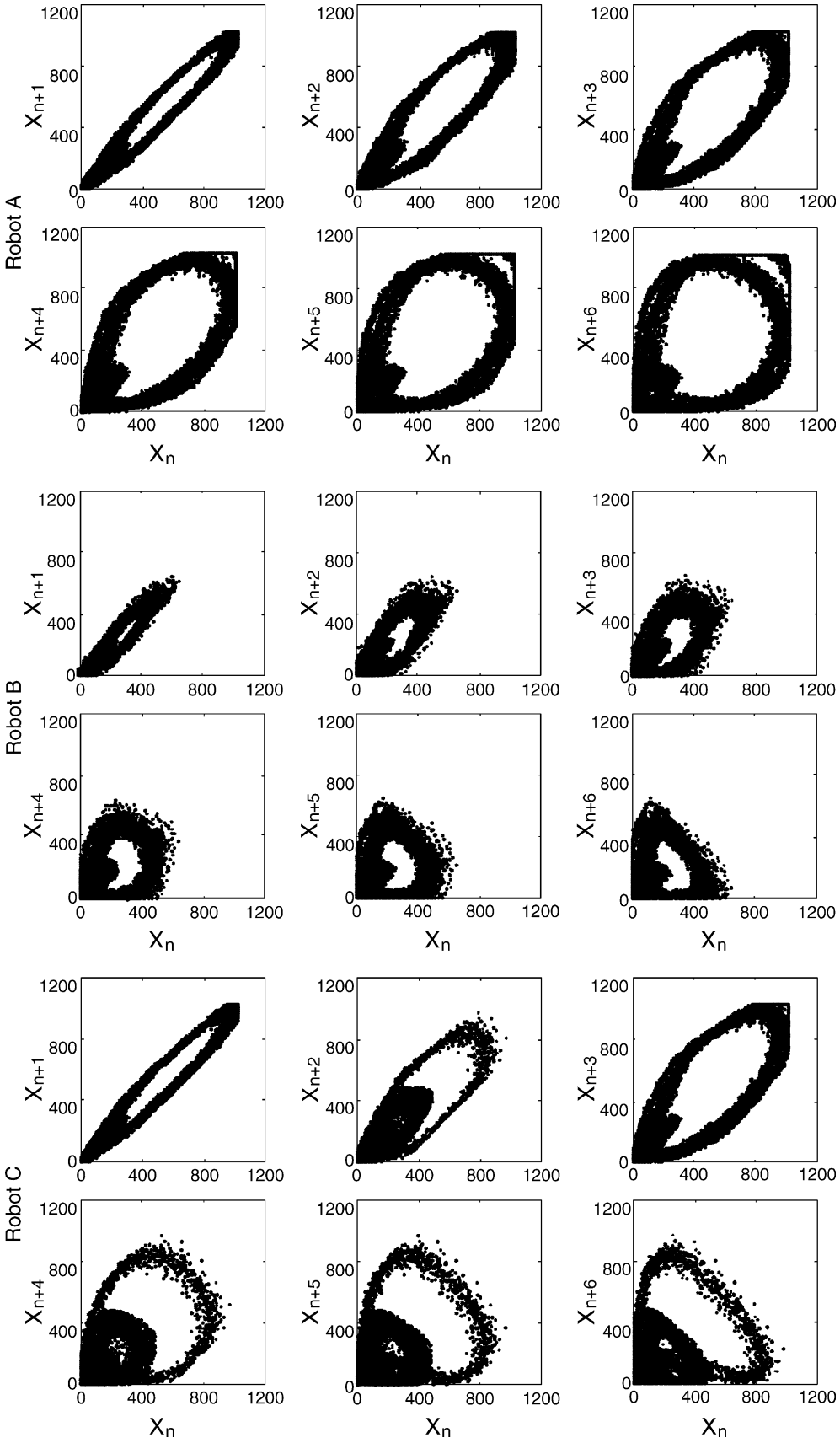

Fig. 8. Return maps for three robots in the Maze environment.

environments, for different values of τ ranging from 1 to 6, are shown in Figs. 8 and 9, respectively. The pattern of the return map was very consistent among fifteen trials for each robot in any of the test environments. Here, each return map was drawn without lines between points for clarity. However, the data traveled along the oval shape of the trajectory in any sensory information, and never jumped across the center part of the oval shape such as from the lower limb of the oval shape to the upper.

The dynamic structure of each neighboring data point is revealed by the return map. This structure was almost unique for each robot, as was seen in Fig. 8. For example, the trajectories for robot A exhibited two components: an outer oval shape and the inner gathering of points. The shapes of both components differ from each other among the robots. The presence of a unique trajectory on the return map indicates the existence of the deterministic dynamics behind each of the measured time series (Holden, 1986; Jackson, 1989; Lorenz, 1994; Ott, 1993; Yamaguchi et al., 1999).

Fig. 10 shows the return maps obtained in four different environments by the three robots, which were plotted by using selected values of τ. Each return map exhibited a unique trajectory, indicating the presence of the deterministic rule behind the time series. The pattern of the return map was very consistent among fifteen trials for each robot in any of the test environments. The choice of delay parameter τ plays an important role for describing the dynamics of return maps. If the delay is too short, then X_n is similar to $X_{n+\tau}$, and when they are plotted, all of the data stay near the line of $X_n = X_{n+\tau}$. If the delay is too long, then the coordinates are essentially independent and no information can be gained from the plot.

In this study, the method of mutual information I was used to determine the delay parameter τ for plotting the return map (Fraser, 1989; Fraser & Swinney, 1986). It represents the amount of uncertainty of $X_{n+\tau}$ reduced by the measurement of X_n, or the amount of information on the average predicted about $X_{n+\tau}$ given a measurement of X_n (Fraser & Swinney, 1986). That is, by making the assignment $[s,q] = [X_n, X_{n+\tau}]$, $I_\tau = \int P_{sq}(s,q) \log[P_{sq}(s,q)/P_s(s)P_q(q)]\, \mathrm{d}s\, \mathrm{d}q$, where P_s, P_q and P_{sq}, are the probability distributions of s and q, and their joint probability distributions, respectively. In practice, I_τ for a given time series starts very high, and as τ increases, it decreases and then usually rises again. It has been suggested that the value of τ for first minimum of I_τ is suitable for describing the dynamics of the return map (Fraser & Swinney, 1986). The value of I_τ for the first minimum was almost the same value of the third minimum for robot A, and the return map with the value of τ for the latter gave a clear picture. Therefore, we chose the third minimum to select τ for the robot A, which was 5. For the same reason, the second minimums of I_τ were chosen to select τ for robots B and C, which was 3 for both.

3.2. Fractal dimension estimated with correlation integral

Deterministic chaos is characterized by the inability to predict future consequences, a high sensitivity to the initial values, a non-integer fractal dimension, and other features (Jackson, 1989; Kay et al., 1996). Whether or not a time series has the nature of deterministic chaos can be distinguished by various factors. The power spectrum should be continuous, the largest Lyapunov exponent be positive, the autocorrelation function be converged to zero at the infinite time, points in Poincare map be limited within a certain finite space, and so on. Among them, the presence of the fractal dimension of a non-integer value has been considered as the strong evidence for the presence of the deterministic chaos.

The fractal dimension estimated with correlation integral has been proved to give the most accurate estimate from a time series with a limited length (Grassberger & Procaccia, 1983a,b, 1984). In this study, the correlation integral $C_m(r)$ of one-dimensional time series is calculated according to sphere counting method proposed by Grassberger and Procaccia (Grassberger & Procaccia, 1983b). In this method, the $C_m(r)$ is calculated by constructing spheres around fixed points X_i and counting the number of points X_j in the spheres. The m-dimensional correlation integral $C_m(r)$ is defined by the following equation.

$$C^m(r) = \lim_{N\to\infty} \frac{1}{N^2} \sum_{i,j=1, i\neq j}^{N} \Theta(r - |X_i - X_j|) \tag{5}$$

where Θ is the Heavy-side function. $\Theta = 0$ if the argument is less than zero, otherwise $\Theta = 1$. X is the m-dimensional vector constructed by the embedding of the time series. When the $C_m(r)$ is in proportional to r^d, the scaling factor d, which is a function of m, is called the correlation factor. In practice, the value of d is obtained as a slope of a log $C_m(r)$ vs. log r plot. If d converges to a certain value when m is increased, the value is called the correlation dimension (D), which gives an estimate of the fractal dimension of the time series (Timmer, Haussler, Lauk, & Lucking, 2000).

Figs. 11–13 illustrate examples of log $C_m(r)$ vs. log r plot and d vs. m plot for each of twelve sensory information time series, obtained in four different environments by three robots. Each sensory information consisted of 30720 points of data sampled every 0.1 s. It has been shown that the minimum number of data points ($N_{\min}$) required to obtain a reliable estimate of D is $N_{\min} > \sqrt{2}(\sqrt{27.5})^D$ (Hong & Hong, 1994). That is, $N = 204$ for $D = 3$, $N = 1069$ for $D = 4$ and $N = 5609$ for $D = 5$. In fact, our preliminary experiments to estimate dimension from various lengths of data ($N = 500$, 1000, 2000, 5000, 10,000) have shown that data length over 5000 gave similar estimates of the dimension. Smithers (1995) has used the data length of about 1600 points for $D = 4.2$ in a similar study. Therefore, we think that the length of data (30720 points) used in this study for calculating fractal dimension was sufficient.

The dynamic range of the sensory information was 0 to 1447 ($=1023 \times \sqrt{2}$), but the actual peak magnitude ranged from approximately 200 to 950 (see Fig. 7), with environmental noise of several bits. Therefore, the range

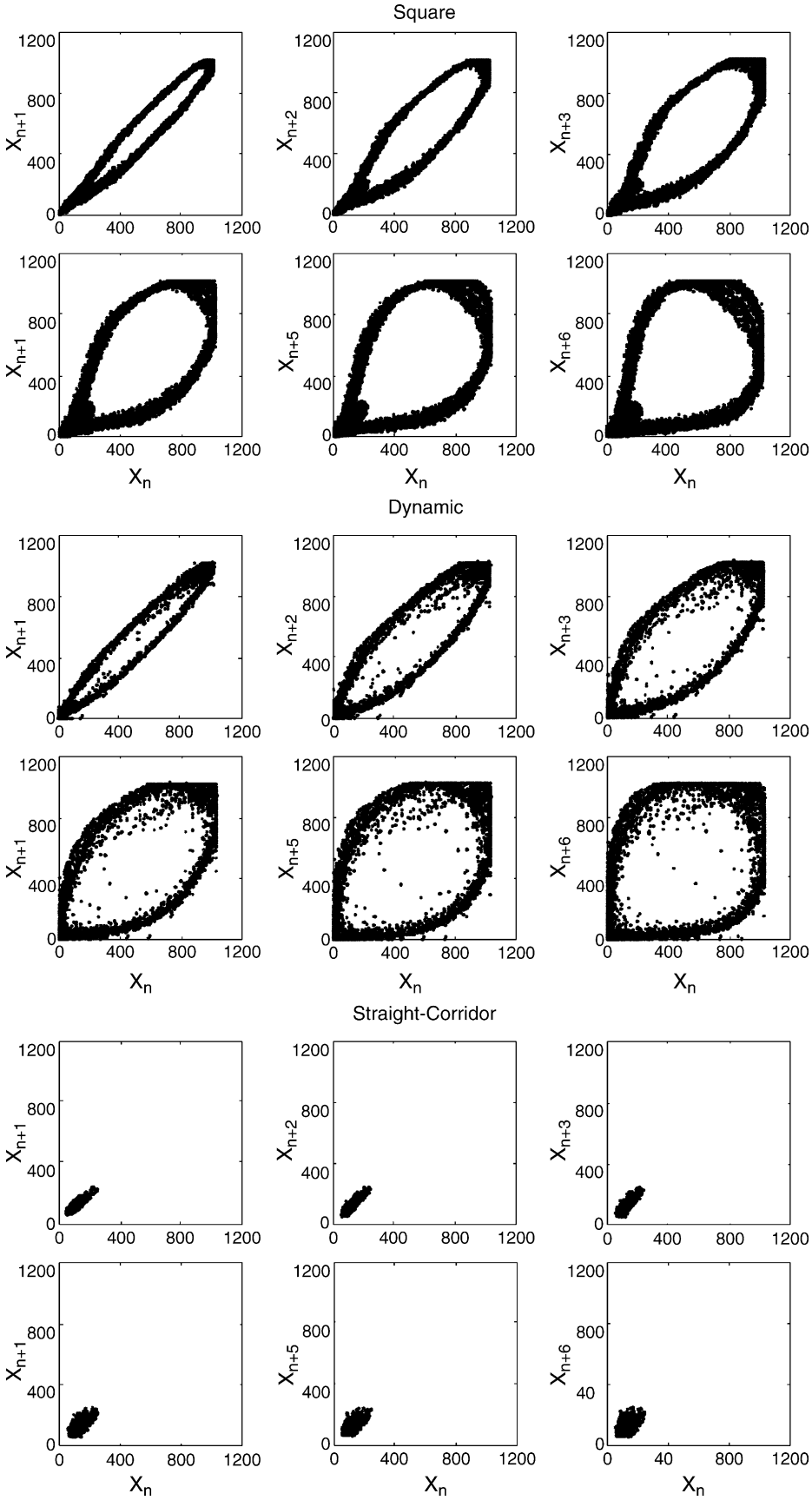

Fig. 9. Return maps for robot A in three different environments.

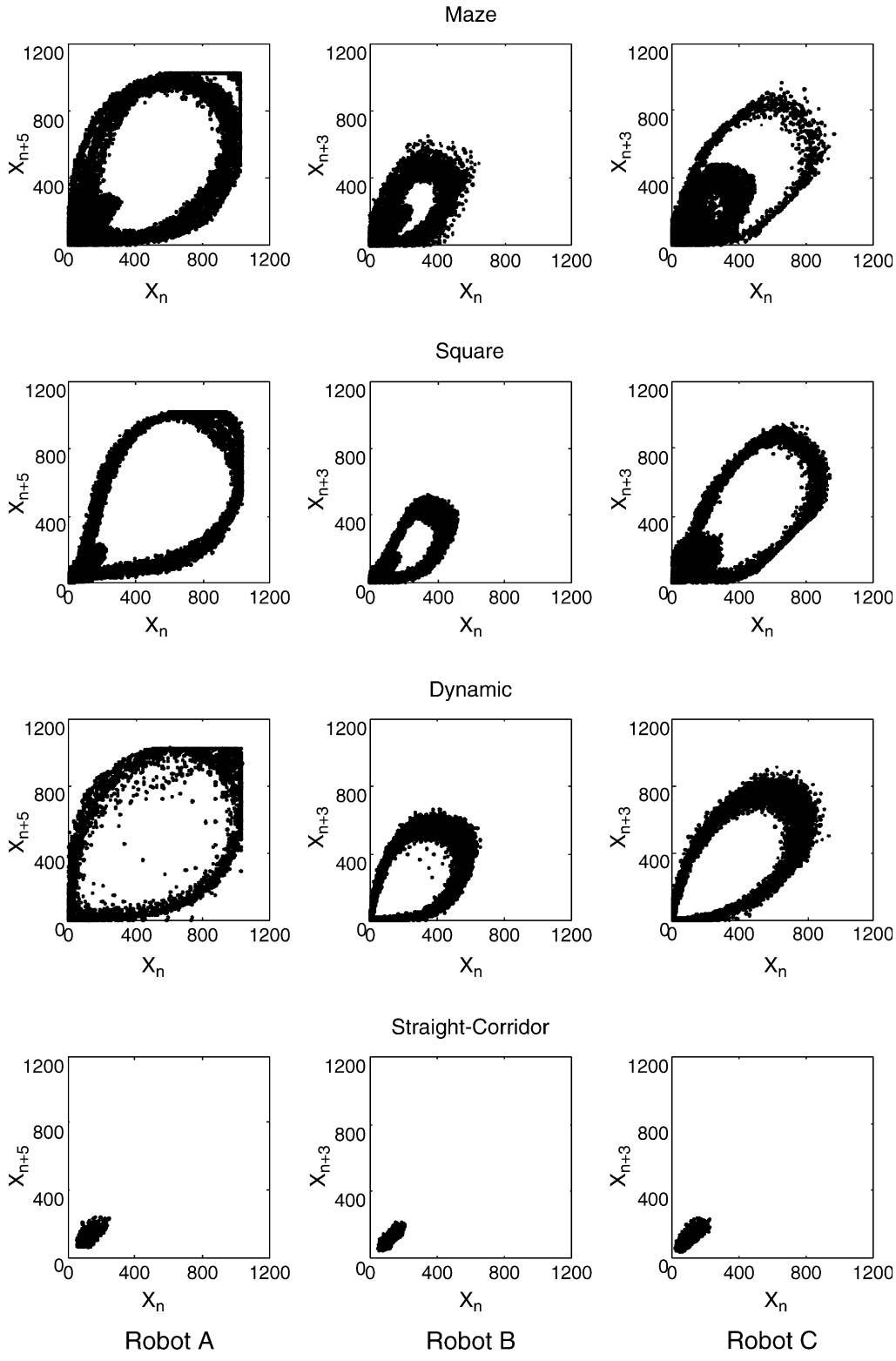

Fig. 10. Return maps for three robots in four different environments.

of log r was set as 0.5 ($\approx$log 3) to 2.5 ($\approx$log 300). The embedding dimension m was chosen to be 2 to 8, i.e. 0.2 to 0.8 s, because less than 1 s seemed to be reasonable for the robot to induce a reflective behavior, considering a navigation speed of approximately 5 cm/s. The graphs were very consistent among fifteen trials for each robot in any of the environments.

In all the graphs of correlation integrals, there were some regions where log $C_m(r)$ increased linearly against log r. That is, there existed scaling region of r for any m.

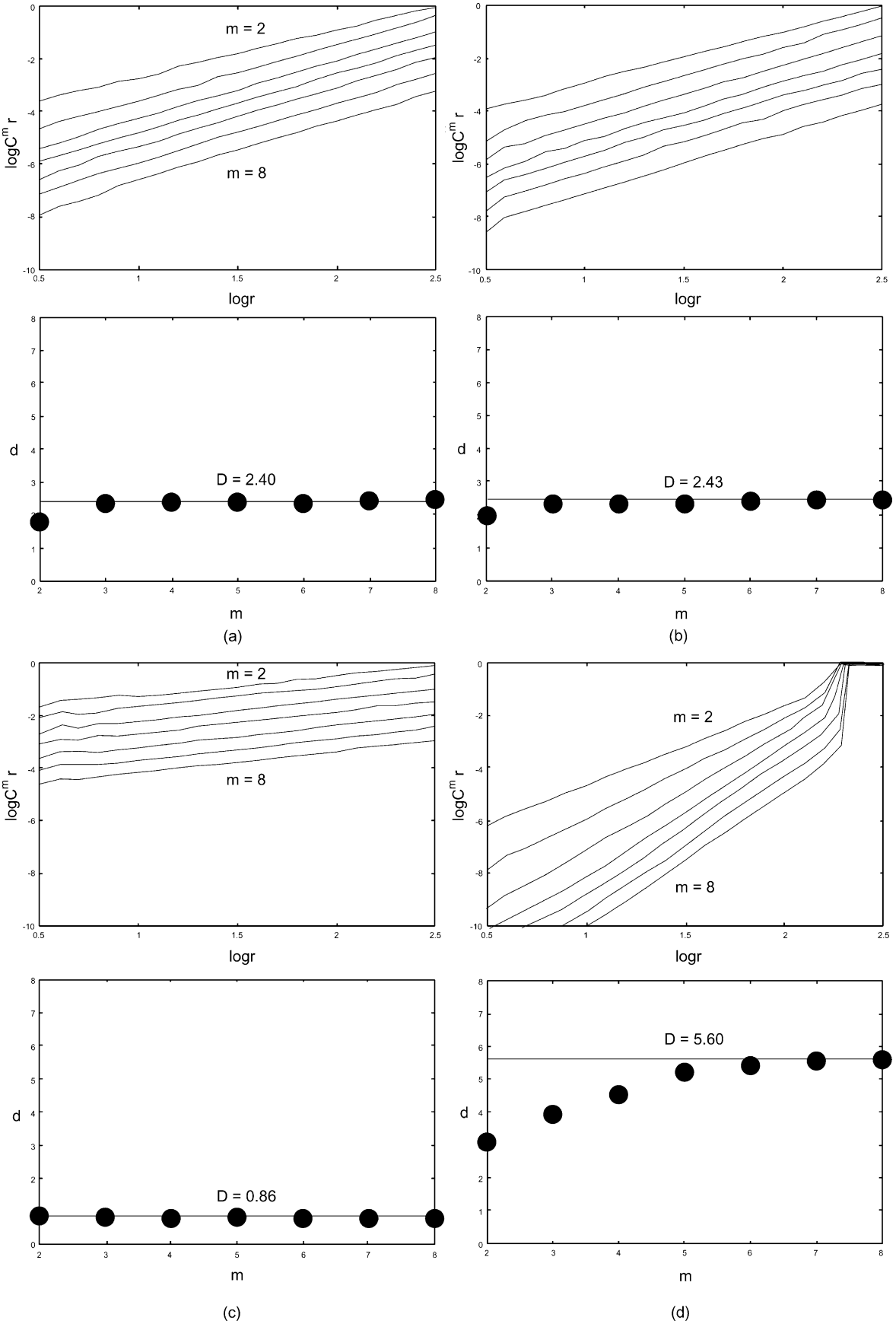

Fig. 11. Correlation integrals of the time series and their slopes for robot A in (a) Maze, (b) Square, (c) Dynamic, and (d) Straight Corridor environments.

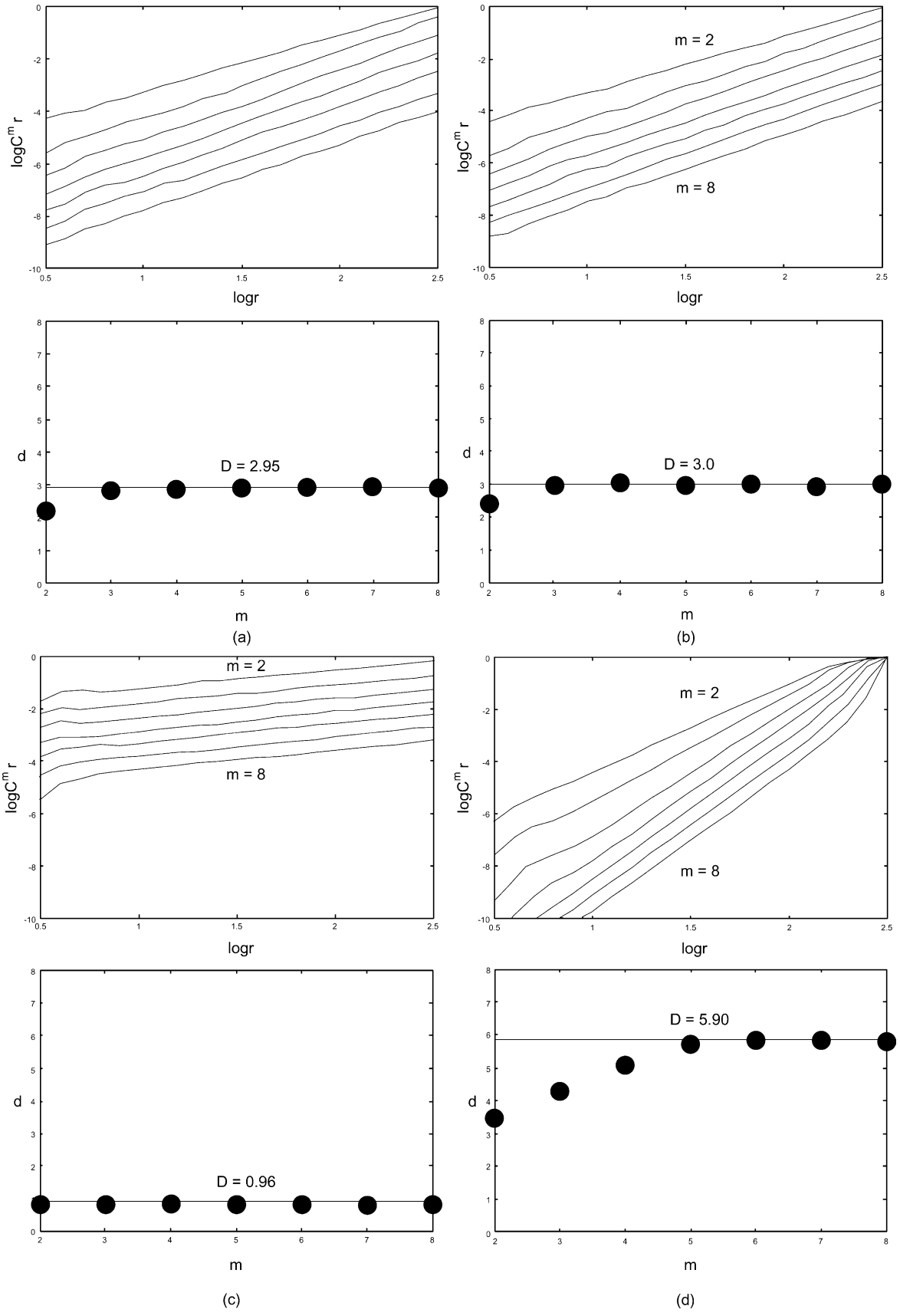

Fig. 12. Correlation integrals of the time series and their slopes for robot B in (a) Maze, (b) Square, (c) Dynamic, and (d) Straight Corridor environments.

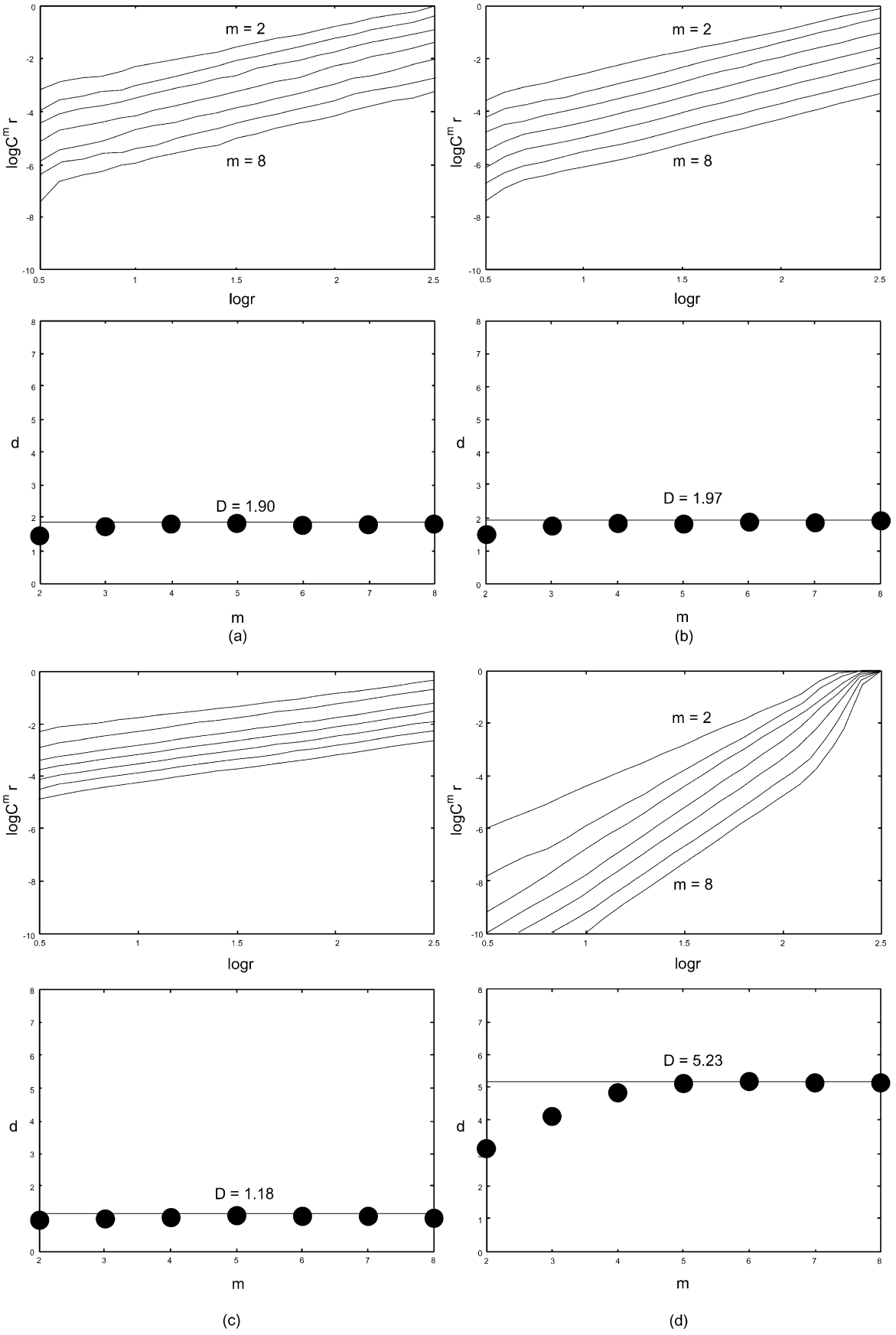

Fig. 13. Correlation integrals of the time series and their slopes for robot C in (a) Maze, (b) Square, (c) Dynamic, and (d) Straight Corridor environments.

The range of log r in which the linearity was held varied among sensory information. The scaling regions were selected by visual observation of plots, as wide as possible within the signal's dynamic range ($0.5 \leq \log r \leq 2.5$). For example, the range was approximated to be 0.5–2.5 for robot A in Maze, 1.0 to 2.5 for robot B in Square, and so on. In most cases, it was linear at least for one log scale of r, i.e. a 10-times range of r, as seen in Figs. 11–13.

The slope, i.e. the scaling factor d, was calculated by fitting a straight line on the log $C_m(r)$ vs. log r plot by the least-mean-square method within the linear range. The scaling factor d converged to a certain value when m increased. For example, d converged to 2.37, 2.57, and 1.88 in the Maze environment for robots A, B, and C, respectively. In order to assure the convergence of d, we calculated the values of d at $m=12$. These values were 2.41, 2.95 and 1.89, respectively, for robot A, B and C in the Maze environment. The values at $m=12$ for Square, Dynamic and Straight-corridor environments were also similar to the ones at $m=8$. These results strongly indicate that these time series have self-similarity in a certain range of r, and there exist the fractal dimensions of non-integer, non-negative values. The presence of the scaling range and the convergence of the slopes have been considered strong evidence for the existence of chaos in a time series (Aihara et al., 1990; Grassberger & Procaccia, 1983a,b; Holden, 1986; Ikeguchi et al., 1990; Jackson, 1989; Lorenz, 1994; Ott, 1993).

In order to assure the estimation of fractal dimension, we did 15 trials for each robot in each environment. Table 1 summarizes the fractal dimensions of three robots in four different environments. For each case, the average of 15 experimental trials as well as the maximum and minimum values were presented. As apparent in the results shown in Table 1, the variations among trials were very small. Therefore, we believe that the estimated dimension reflects well the physical chaotic phenomena, not too much contaminated with environmental and quantum noise.

3.3. Lyapunov exponent

Another common tool for detecting chaos in experimental data is the Lyapunov exponent (λ) λ is a quantitative measure of the sensitivity to the initial condition. It is calculated as the average rate of divergence or convergence of two neighboring trajectories. Actually, there is a whole spectrum of λs; for a system with N variables, there are $N\lambda$s.

Table 1
Correlation dimensions for three robots in four different environments

Robot		Environment			
		Maze	Square	Dynamic	Straight-Corridor
A	Min	2.35	2.40	0.81	5.54
	Avg	2.41	2.49	0.87	5.70
	Max	2.52	2.60	0.95	5.85
B	Min	2.90	2.96	0.90	5.87
	Avg	3.01	3.07	0.94	5.96
	Max	3.14	3.20	1.03	6.07
C	Min	1.86	1.88	1.10	5.23
	Avg	1.92	1.95	1.16	5.29
	Max	2.03	2.05	1.23	5.35

The results were averaged over 15 independent runs.

To obtain the Lyapunov spectra, imagine an infinitesimal small ball with radius dr sitting on the initial state of the trajectory. The flow will deform this ball into an ellipsoid. That is, after a finite time t all orbits, which have started in that ball, will be in the ellipsoid. The ith λ is defined by

$$\lambda_i = \lim_{t\to\infty} \frac{1}{t} \frac{dli(t)}{(dr)} \tag{6}$$

where dl_i is the radius of the ellipsoid along its ith principal axis.

For a conservative (Hamiltonian) system, this quantity is zero. For a dissipative system, the quantity is negative and there exists an attractor for the dynamics toward which initial conditions in the basin of attraction are drawn. If the system is chaotic, at least one of the λs must be positive, and a strange attractor will exist. This means that the local exponential divergence of nearby trajectories in chaotic systems lead to sensitivity of the trajectories against small changes in the initial values.

The usual convention of ordering the λs is from the largest (most positive) to the smallest (most negative). For a chaotic system, the largest Lyapunov exponent λ_1 must be positive. If one speaks about the Lyapunov exponent, generally the largest one is meant. Different algorithms have been proposed to estimate the largest Lyapunov exponent or even their complete spectrum from measured data. In this study, we calculate λs of the sensory information according to Kaplan & York (1997); Oseledec (1968); Shimada & Nagashima (1979), and Wolf, Swift, Swinney, & Vastano (1985).

Kaplan and York (1997) have conjectured that the dimension of a strange attractor can be approximated from the spectrum of λs. Such a dimension has been called the Kaplan–Yorke (or Lyapunov) dimension, and it has been shown that this dimension is close to other dimensions such as the boxcounting, information, and correlation dimensions for typical strange attractors.

If $S(D)$ represent the sum of the exponents from 1 to D where $D<N$, then it is evident that for a strange attractor, there is some maximum integer $D=j$ for which S is positive and an integer $j+1$ for which S is negative. The attractor must then have a fractal dimension that lies between j and $j+1$. The essence of the Kaplan–Yorke conjecture is simply to interpolate the function $S(D)$ and evaluate the value of D for which $S=0$. That is, we seek the hypothetical fractional dimension in which there is neither expansion nor contraction. Using a linear interpolation, this value is

$$D_{\mathrm{KY}} = \frac{j - S(j)}{\lambda_{j+1}} \tag{7}$$

where D_{KY} is known as Kaplan–Yorke or Lyapunov dimension.

Table 2
Examples of Lyapunov spectra and Kaplan–York dimension for robots A, B and C in four different environments

Lyapunov spectra/ dimension	Maze			Square			Dynamic			Straight-Corridor		
	A	B	C	A	B	C	A	B	C	A	B	C
λ_1	0.47	0.48	0.31	0.39	0.46	0.25	0.15	0.13	0.12	1.48	1.56	1.29
λ_2	0.00	0.09	0.00	0.00	0.11	0.00	−7.69	−4.37	−6.67	0.95	0.98	0.97
λ_3	−2.10	0.00	−9.74	−1.33	0.00	−8.87				0.38	0.67	0.41
λ_4		−5.72			−16.32					0.12	0.33	0.19
λ_5										0.00	0.14	0.00
λ_6										−3.89	0.00	−8.58
λ_7											−6.19	
D_{KY}	2.22	3.10	2.03	2.29	3.03	2.03	1.02	1.03	1.02	5.75	6.59	5.33

Numerical experiments to determine Lyapunov exponents were performed around the regions where correlation dimensions were obtained. Embedding dimensions of reconstructed state space were chosen within the ranges where the slope d of correlation integral, such as Fig. 11–13, converged. They were; 3–4 for Maze and Square environments, 1–2 for Dynamic environment, and 5–7 for Straight-Corridor environment. Reconstruction time delay was chosen to be 5–7 for robot A and 3 for robots B and C in accordance with the results on mutual information described in Section 3.1. The mean number of replacement points located in a region of length and the angular size were 5–7 and 0.2–0.5 radians, respectively. These parameter values were used after some preliminary experiments for each time series to make sure that small changes in the parameter values did not make significant changes in estimated values of Lyapunov exponents. To locate the nearest neighbor to the first point (the fiducial point), the replacement strategy as suggested by Wolf et al. (1985) was used.

In order to estimate reliable Lyapunov exponents, fifteen sets of numerical experiments were performed in each of twelve conditions, in four different environments for three robot types. Table 2 shows examples of Lyapunov spectra obtained in one set of experiments as well as of Kaplan–Yorke dimensions D_{KY} calculated from the Lyapunov spectra. In any of the conditions, Lyapunov exponents were converged and λ_1s were positive, which is an indication of chaos. Lyapunov spectra were fairly consistent in fifteen trials, possibly owing to sufficiently long data length (N= 30720 points) of each time series. Average values of the largest Lyapunov exponents and D_{KY}s over fifteen sets of experiments are presented in Table 3.

3.4. Behavioral performance and fractal dimension

Analysis of sensory information by dynamical system perspective has been introduced to the robotics community for nearly a decade. However, the aim of the most analysis is to determine the chaotic property in the sensory information of autonomous robots. It has been not known whether this property correlate to the performance of robots. The aim of this subsection is to find out the relation between the fractal dimension and the performance measure of robots.

A new set of experiments has been carried out to calculate fractal dimensions at various stages of evolutionary process in three different robots. In these experiments, robots A, B and C were evolved in the maze environment for 50 generations, and their performances, measured by the fitness function (Eq. (2)), were recorded during the course of evolution. Evolved robots in different generations were then tested in the same environment for collecting sensory information. Fractal dimension estimated with correlation integral, described in Section 3.2, was then used to determine the degree of chaos generated for evolved robots at different generations.

Fig. 14 shows fitness values and fractal dimensions of robot A, B and C at different generations. It can be observed from Figs. 14(a) and (b) that the degree of chaos generated as well as the performance of robots were increased along the course of evolution. For robot A, for example, the fitness value and fractal dimension at generation 10 were 0.05 and 0.25, respectively, while the fitness values and fractal dimension were 0.10 and 0.57, respectively, at generation 20. This indicates that the performance of robots increases when the degree of chaos increases. In other words, higher degree of chaos helps to produce behavior that fits better to the given environment.

Table 3
Largest Lyapunov exponents and Kaplan–York dimensions for robots A, B and C in four different environments

Robot		Environment			
		Maze	Square	Dynamic	Straight-Corridor
A	λ_1	0.35	0.32	0.10	1.41
	D_{KY}	2.43	2.46	1.03	5.65
B	λ_1	0.41	0.39	0.13	1.48
	D_{KY}	3.05	3.09	1.07	6.01
C	λ_1	0.26	0.28	0.11	1.37
	D_{KY}	1.96	2.02	1.12	5.25

The results were averaged over 15 independent runs.

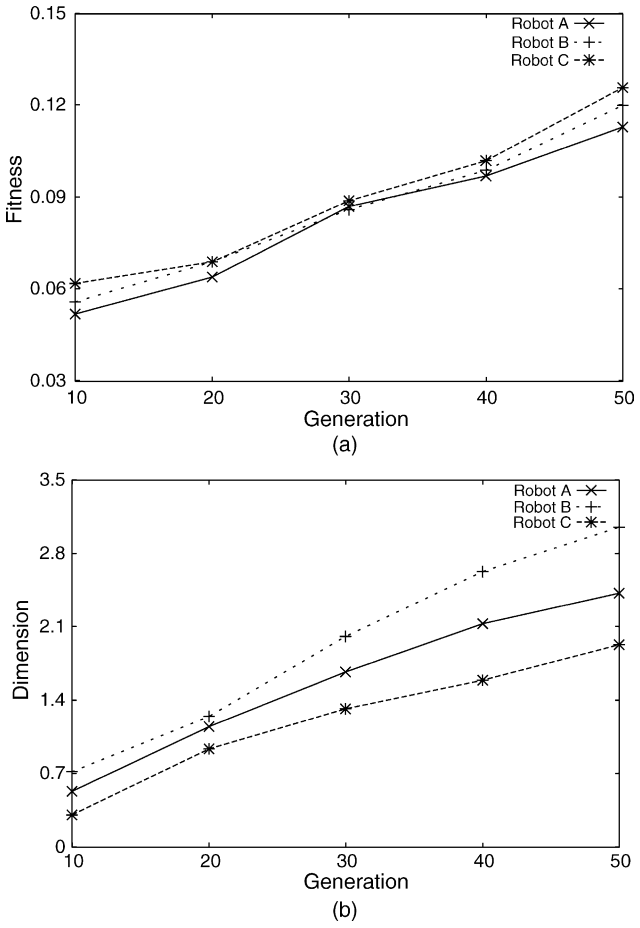

Fig. 14. (a) Fitness value and (b) Fractal dimension, for robots A, B and C at different generations in the Maze environment.

4. Discussion

There have been a number of studies to describe the interaction between an autonomous robot and its environment as a dynamical system (e g., Beer, 1995; Smithers, 1995; Tani, 1996). Some studies have aimed to exhibit the presence of deterministic chaos in the internal state(s) of an autonomous robot navigating in an environment (e.g. Smithers, 1995). It has been shown that the return map of sensory information obtained during a free navigation in an environment, as well as fractal dimension and Lyapunov exponent calculated from it, is consistent in 15 trials. However, as of our knowledge, none so far has actually exhibited how the environment affects the dynamics, specifically the chaos dynamics, of an autonomous robot interacting with the environment. This is, we believe, important because it will help to understand how the autonomous robot solve problems associated with environmental changes. And also, it has not been demonstrated well how the control architecture and the chaotic property of the robot affect the behavioral dynamics and performance. This is essential in practice for the optimal design of autonomous robots as well as for understanding the autonomy. In order to obtain good estimates of fractal dimensions of time series, it is necessary to have a certain long period of recording. We utilized a miniature mobile robot that allowed reproducible experiments with a sufficiently long duration.

In this study, we analyzed the sensory information perceived by a mobile robot having different controller in four different environments as complex systems. In Section 4.1, the implications of the analysis described in Section 3.4 are discussed from four points of view: (1) how the regularity in the sensory information differs among individuals, (2) how the environment affects regularity, (3) how behavioral changes are induced by sensory information, and (4) the degree of complexity of the task given to the robot.

4.1. Individual differences revealed by trajectory of return map

While the behavior of robots in any of the tested environments appeared much alike in terms of visual observation, there were clear differences in trajectory on the return map That is, all three types of robots navigated well at a similar speed in any environment, and with a similar capability to avoid obstacles. This was evidenced by the results showing that the patterns of sensory information were quite alike among the robots, except that the magnitudes of sensory signals differed from each other (Figs. 4 and 5), reflecting the possible difference in the distance of several millimeters from the wall. Their fitness values as well as their evolution processes were also similar to each other (Fig. 3). Thus, these conventional measures are incapable to distinguish these robots. However, as apparent in Fig. 8, there were considerable differences among the robots in regard to the trajectory pattern on the return map, though they were genetically evolved in an identical environment (Fig. 2). Environmental changes given to each robot made much less difference in the trajectory pattern in contrast (Figs. 9 and 10).

As was seen in Fig. 10, the difference on the return maps obtained in two environments, the Maze and Square, was marginal for each of the robots; at least the difference caused by the environmental change was far less than the differences among robots. These results indicate that the perception, or the way the world is seen through the sensory organs of the autonomous robot, is characteristic to each robot, and the return map of the sensory information can exhibit the characteristics as the change in the trajectory pattern.

It might be appropriate to emphasize here that the mobile robot used two front sensors 1 and 4 to generate the motor outputs and thus its behavior, and that the sensory information was also constructed from the values form sensors 1 and 4. In other words, the behavior was monitored by the sensors, which were located on the robot, i.e. from the coordinate of the robot. Therefore, one could argue that

the sensory information was not the cause for the behavior, but the result. In fact, we could have used all of eight proximity sensors all around the robot's body to generate motor outputs, and observed the behavior with two front sensors. However, in the behavior-based robotics, the sensor signals are also the cause of behavior (Brooks, 1986). In this study especially, exactly the same sensory signals were used for both generating and observing behavior. Thus, the flow of information through the sensory organs of the robot used in this study should contain all the information necessary to generate the behavior.

We reduced the two-dimensional sensory information down to a one-dimensional time series that represents the distance to the front obstacle, and that sensory information exhibited a characteristic dynamics on the phase plane. Therefore, we may say conversely that the robot has evolved to behave so as to maintain the sensory information on the trajectory. The intelligence of the robot necessary to perform the task of navigating with obstacle avoidance is expressed by the regularity of the trajectory at least in part. In other words, a portion of the behavior-based intelligence of the robot is present in the flow of sensory information expressed as the trajectory's regularity.

4.2. Trajectories specific to certain environments

The next question we asked was how the perception of each individual changes in various environments We placed three robots in four different environments, the Maze, Square, Dynamic and Straight-Corridor, with the return maps of the sensory information illustrated in Fig. 10. In all the maps, characteristic patterns in the trajectory could be seen; that is, a unique regularity was present in each of the sensory information.

In case of robot A, an outer and inner component can be seen in the trajectory on the return maps obtained in the Maze and Square environments. While the inner component was composed during navigation in the environments' straight paths, the outer component was due to the avoidance of the head-on collision at the corners, where larger sensor signals and dynamical moves were elicited than in the straight path. On the return map, thus, transitions from the inner part to the outer occurred when the robot encountered every corner after navigating the straight path. In the Dynamic and Straight-Corridor environments, only the outer and inner components could be seen, respectively. This is reasonable because the former elicited only obstacle avoidance behavior, while the latter elicited navigation in a straight path.

In case of robot B, the outer component on the return map was smaller than that obtained in robot A. That is, robot B behaved in a manner similar to robot A except that it was a bit far from any obstacles, probably by several millimeters, as evidenced by the smaller magnitude of sensory information (Fig. 4).

In case of robot C, there is an inner component in the Square environment, while in the Maze environment there seems to exist another, larger inner component in addition to the one observed in the Square environment. This is probably due to the asymmetry of connection weights. That is, in the Maze environment, the robot had to make both left and right turns. In contrast, in the Square environment it needed only one of them because it had to make only one directional turn. Therefore, robot C has three different trajectories, one for moving straight corridor and two for avoidance of front obstacles.

These results could indicate that each robot behaves in such way that the flow of sensory information becomes constant even when the environment changes. In other words, each robot might see the world in its own way irrespective of environmental differences. This hypothesis is argued further in Section 4.3.

4.3. Transition in trajectory induced by environmental change

If the robot behaves in such a way that it maintains a constant flow of sensory information, what would happen when the sensory information is insufficient to maintain the consistency of the flow? This condition is certainly possible when the surrounding environment of the robot changes drastically so that the sensor signals can no longer contain the information necessary to maintain the regularity of the flow

In the Straight-Corridor and Dynamic environments, which shared no similarity, the trajectories on the return map obtained in these environments were totally different each other (Fig. 10). In the Maze and Square environments, which contain straight paths and right-angled corners, the trajectory was similar in both of the environments: The trajectory consisted of inner and outer components. Fig. 10 shows that these two components were similar to the ones obtained in the Straight-Corridor and Dynamic environments, respectively.

These results can be interpreted as follows. The behavior-based robot is behaving in such a way as to maintain a consistency in the flow of sensory information. But when the environment changes drastically and the flow of sensory information can no longer maintain this consistency, a transition to another trajectory that is sufficient to maintain another consistency takes place. Both of the environments, the Square and the Maze, consisted of two sub-components, straight paths and corners. For when the robot traveling along a straight path suddenly encounters a corner, wherein the previous strategy to maintain the flow of sensory information constant is no longer valid, another strategy should be used to avoid a head-on collision. In other words, a transition of the sensory information flow should occur when the robot encounters a new environment. A new strategy or new pattern of sensory information flow should already have been acquired within the network during the evolutionary process. There should be thus at least two components in the sensory information flow, and they are the ones apparent on the return map; they are the inner and outer components.

In summary of Sections 4.1–4.3, we have analyzed the sensory information regarding freely moving real autonomous robots in environments. This is, of our knowledge, the first clean demonstration showing the effects of environment and controller on the internal state dynamics of fully autonomous robots. We demonstrated that regularity is present in the return map of the sensory information, and that it can be divided into substructures, each of which corresponds to a specific behavioral pattern. In the environment in which one of the behaviors is predominant, the return map exhibited only the corresponding substructure; that is, transitions from one state to other are occurring during the autonomous behavior in response to sensory information. Such transitions of the internal state seem analogous to the phenomena reported in the brain that has been considered as the source of the intelligence (Degn et al., 1997; Freeman, 1991, 1994; Kay et al., 1996). In the brain, chaos, however, the state tends to transits from one local attractor to another rather autonomously in various ways. The robots in this series of experiments do not exhibit such autonomy of generating diversity since the mapping between the environment situation and the internal dynamic structure is simply one to one mapping. In this study, robot transits one chaotic state to the other in response to environmental changes. This is a good contrast to the Tani's work (Tani, 1996), where robot is made to transit one non-chaotic state to the other and chaos takes place at the transition, i.e. at the time of decision making.

4.4. Complexity of tasks

The fractal and Lyapunov dimensions obtained for various sets of sensory information are shown in Tables 1 and 2, respectively. The values of fractal dimension that was estimated with correlation integral are quite similar to the ones of Lyapunov dimensions. For all the types of robots used in the present study, the fractal dimensions in the Maze environment is quite similar to that in the Square environment. This is reasonable because the Square environment consists of parts similar to those of the Maze environment, i.e. straight paths and right-angled corners. The small variations might be done to the fact that the locations of obstacles in environments varied by at most ± 3 mm, and the Square environment could not be exactly the sub-environment of the Maze environment. In the Dynamic environment, the dimension is much lower. It is also reasonable because the robot's task is only to avoid front obstacles by generating reactive rotation, which is much easier than other tasks.

It is most interesting that the dimension is highest in the Straight-Corridor environment. This was common to all the robot types. We interpreted this as follows. In Straight-corridor environment, there is a tight coupling between environment and robot. The behavior of the robot is generated by the sensory information from sensors 1 and 4, and the sensors are always sensing the walls of both sides in environment. By using the sensory information, the robot has to generate behavior that is sufficient to maintain itself at the center of the corridor and to move forward through the narrow corridor. In contrast, in Dynamic environment, the task for the robot is to avoid head-on collision by simply generating rotating behavior. After avoiding the obstacle in front, there is no obstacle for a moment and it is allowed to move any direction freely. The coupling with the environment thus only occurs at the time when the robot faces an obstacle in front. On first glance, the navigation in the straight path appears the easiest to perform. It is, however, very difficult for the robot to maintain itself at the center of the corridor or to follow the wall along a side, much like walking on a log bridge.

Furthermore, as evidenced in Table 3, robot with higher fractal dimension tends to exhibit higher fitness value. This suggests that higher order of chaos helps the robot to become more adaptive to environmental changes encountered during the course of behavior.

In summary of Section 4.4, we have estimated the correlation and Lyapunov dimensions of sensory information obtained in a robot with three different controllers. This is the first attempt to actually exhibit the effect of controllers, environments and performance on the dimension in real robot as of our knowledge. The estimated values of the dimensions seem to correspond well to the tasks given to the robot and the performance. The dimension value could be used as a measure of the difficulty of the task for the robot. It should be kept in mind that the measure is only from the view point of the specific individual. The evaluation might vary among individuals with different experiences, such as those who have evolved in different environments.

5. Summary and conclusion

In order to study the regularity and complexity of autonomous behavior, the flow of sensory information in autonomous mobile robots was analyzed as a complex system. We used a miniature mobile robot, in which motor outputs were generated by proximity-sensor signals by means of a two-layered artificial neural network. The weights were determined by the genetic evolution necessary to navigate and avoid obstacles in the "Maze" environment, which consisted of straight corridors and right-angled corners. During the autonomous navigation of the best individual, sensor signals were collected, and one-dimensional sensory time series representing the proximity to obstacles in front of the robot was constructed.

The sensory time series X_n, which appeared random, was plotted on the return map, the plot of $X_{n+\tau}$ vs. X_n. The trajectory exhibited a unique structure, representing the underlying regularity of the time series. Correlation integral analysis further confirmed that the sensory time series expressed some properties of deterministic

chaos—the presence of scaling regions and a finite embedding dimension. The same analysis was performed on two other robots having different network topologies or structures. Trajectories on return maps differed among robots. In contrast, when each robot was placed in a simple square-shape path, the trajectories were identical to those obtained in the Maze environment. These results indicate that an autonomous robot behaves in such a way that the flow of sensory information becomes constant, and that the pattern is characteristic to each robot.

For all the robots, there existed two trajectory components corresponding to the navigation of a straight corridor and corners. Experiments conducted in the Straight Corridor, and in the Dynamic environment where only head-on collisions were manually given, confirmed that transitions from one trajectory to another occur during the course of autonomous behavior. This observation suggests that the autonomous robot under no constraints behaves in a such a way that the sensory information flow travels on a chaotic attractor having multiple substructures. Jumping from one sub-attractor to another allows adaptation to new environments. Such transitions might be the source of intelligence in generating adaptive behavior as was found (Degn et al., 1997; Freeman, 1991, 1994a) and analyzed in the brain (Freeman, 1994b; Kay et al., 1996).

The fractal dimension is used in this study to quantify the complexity of autonomous behavior and the relative difficulty of tasks for three types of robots in four different environments. For all robots, the fractal dimension in the evolved (i.e. Maze) environment is similar to that obtained the unknown (i.e. Square) environment consisted of the same sub-environments. However, the highest and lowest fractal dimensions were obtain for the Straight-Corridor and Dynamic environments, respectively. This was common for all the types of robots. This is also reasonable because robots need to avoid only head-on collisions in Dynamic environment, while they have to continuously maintain themselves at the center of the narrow path in the Straight-corridor environments by keeping a tight coupling with environment through the sensory information. Therefore, the fractal dimension could be utilized to quantify the difficulty of the task given to the robot, and to compare the controllers of the robot. In addition, we have shown that the dimension could be utilized as the performance measure.

These studies raise many questions for future works. For example, how the return map and the fractal dimension would be if the robot uses more sensor, how they differ among physically different robots, how robustness correlates with fractal dimension, etc. One of the largest questions would be how we can utilize these results in designing autonomous robot. We are currently working on limiting the robot behaviors in phase space during evolution, so that the unexpected dangerous behavior may not occur and also we are trying to introduce an algorithm that develop a robot with a smaller fractal dimension.

Acknowledgements

Authors thank Drs Takashi Gomi, Dario Floreano, and Takayuki Hirata for their encouragement and discussion, and Drs Ryouich Odagiri and Tatsuya Asai, and Mrs Akira Matsumoto and Hirotaka Akita for their technical assistance. Authors are also very grateful for anonymous reviewers whose comments helped to improve the quality of paper considerably. This work was supported by grants from the Artificial Intelligence Research Promotion Foundation, the Yazaki memorial Foundation and Hokuriku Industrial Advancement Center, and a Grant-in-Aid for Scientific Research from Japanese Society for the Promotion of Science.

References

Aihara, K., Takabe, T., & Toyota, M. (1990). Chaotic neural networks. *Physics Letters A*, *144*(6), 333–340.

Babloyantz, A., & Destexhe, A. (1986). Low-dimensional chaos in an instance of epilepsy. *Proceedings of the National Acadamic Science*, *83*, 3513–3517.

Babloyantz, A., Salazar, J. M., & Nicolis, C. (1985). Evidence of chaotic dynamics of brain activity during sleep cycle. *Physics Letters A*, *111*, 152–156.

Beer, R. D. (1995). A dynamical systems perspective on agent-environment interaction. *Artificial Intelligence*, *72*, 173–215.

Biro, Z., & Ziemke, T. (1998). Evolution of visually-guided approach behavior in recurrent artificial neural network robot controllers. In R. Pfeifer, B. Blumberg, J.-A. Meyer, & S. Wilson (Eds.), *From animals to animats 5: Proceedings of the fifth international conference on simulation of adaptive behavior (SAB98)* (pp. 73–76). Cambridge, MA: MIT Press, 73–76.

Braitenberg, V. (1984). *Vehicles: Experiments in synthetic psychology*. Cambridge, MA: MIT Press.

Brooks, R. A. (1986). A robust layered control system for a mobile robot. *IEEE Transaction on Robotics and Automation*, *RA-2*, 14–23.

Brooks, R. A. (1991). Intelligence without representation. *Artificial Intelligence*, *47*, 139–159.

Degn, H., Holden, A. V., & Olsen, L. F. (1997). *Chaos in biological systems*. New York: Plenum.

Floreano, D., & Mondada, F. (1994). Automatic creation of an autonomous agent: Genetic evolution of a neural network driven robot. In D. Cliff, P. Husbands, J.-A. Meyer, & S. Wilson (Eds.), *From animals to animats 3: Proceedings of the third international conference on simulation of adaptive behavior (SAB'94)* (pp. 421–430). Cambridge, MA: MIT Press, 421–430.

Floreano, D., & Mondada, F. (1996). Evolution of homing navigation in a real mobile robot. *IEEE Transactions on Systems, Man, and Cybernetics—Part B*, *26*(3), 396–407.

Fraser, A. M. (1989). Information and entropy in strange attractors. *IEEE Transactions on Information Theory*, *35*(2), 245–262.

Fraser, A. M., & Swinney, H. L. (1986). Independent coordinates for strange attractors from mutual information. *Physical Review A*, *33*, 1134–1140.

Freeman, W. J. (1991). The physiology of perception. *Scientific American*, *264*, 78–85.

Freeman, W. J. (1994a). Role of chaotic dynamics in neural plasticity. *Progress in Brain Research*, *102*, 319–333.

Freeman, W. J. (1994b). Neural networks and chaos. *Journal of Theoretical Biology*, *171*, 13–18.

Grassberger, P., & Procaccia, I. (1983a). Measuring strangeness of strange attractors. *Physica 9D* , 189–208.

Grassberger, P., & Procaccia, I. (1983b). Characterization of strange attractors. *Physical Review Letter*, *50*, 346–349.

Grassberger, P., & Procaccia, I. (1984). Dimensions and entropies of strange attractors from a fluctuating dynamics approach. *Physica*, *13D*, 34–54.

Hayashi, H., Ishizuka, S., & Hirakawa, K. (1985). Chaotic response of pacemaker neuron. *Journal Physics Society Japenese*, *54*, 2337–2346.

Holden, A. V. (1986). *Chaos*. Priceton: Manchester and Princeton University Press.

Holland, J. H. (1975). *Adaptation in natural and artificial systems*. Ann Arbor: The University of Michigan Press.

Hong, S.-Z., & Hong, S.-M. (1994). An amendment to the fundamental limits on dimension calculations. *Fractals*, *2*, 123–137.

Ikeguchi, T., Aihara, K., Ito, S., & Utsunomiya, T. (1990). A dimensional analysis of chaotic neural networks. *IEICE Journal*, *73-A*, 486–494 (in Japanese).

Jackson, A. E. (1989). *Perspectives of nonlinear dynamics*. Cambridge: Cambridge University Press.

Kaplan, J. L., & York, J. A. (1997). *Chaotic behavior of multidimensional difference equations Lecture notes in mathematics*, Vol. 730. Berlin: Springer pp. 204–227.

Kay, L. M., Lancaster, L. R., & Freeman, W. J. (1996). Reafference and attractors in the olfactory system during odor recognition. *International Journal of Neural Systems*, *7*, 489–495.

Lorenz, E. N. (1994). *The essence of chaos*. University Washington Press.

Matsumoto, G., Aihara, K., Hanyu, Y., Takahashi, N., Yoshizawa, S., & Nagumo, J. (1987). Chaos and phase locking in normal squid axons. *Physics Letters A*, *123*, 162–166.

Mondada, F., Franzi, E., & Ienne, P. (1993). Mobile robot miniaturization: A tool for investigation in control algorithms. *Proceedings of the third international symposium on experimental robotics, Kyoto, Japan*. (pp. 501–513).

Naito, T., Odagiri, R., Matsunaga, Y., Tanifuji, M., & Murase, K. (1997). *Genetic evolution of a logic circuit which controls autonomous mobile robot Lecture Notes in Computer Science*, vol. 1259. Berlin: Springer pp. 210–219.

Nolfi, S., Floreano, D., Miglino, O., & Mondada, F. (1994). How to evolve autonomous robots: Different approaches in evolutionary robotics. In R. A. Brooks, & P. Maes (Eds.), *Proceedings of the IV International Workshop on Artificial Life* (pp. 122–133). Cambridge, MA: MIT Press, 122–133.

Odagiri, R., Monirul Islam, Md., Okura, K., Asai, T., & Murase, K. (1999). Deterministic chaos in sensory information of real mobile robot Khepera. In A. Loffler, F. Mondada, & U. Ruckert (Eds.), *Experiments with the mini-robot Khepera: Proceedings of the first international Khepera workshop* (pp. 49–56). Paderborn, Germany: HNIVerlangss-chriftenreihe, 49–56.

Odagiri, R., Wei, Y., Asai T., & Murase, K. (1998). Measuring the complexity of the real environment with evolutionary robot: Evolution of a real mobile robot Khepera to have a minimal structure. *Proceedings IEEE International Conference on Evolutionary Computation Anchorage, USA*. (pp. 348–353).

Odagiri, R., Wei, Y., Asai, T., Yamakawa, O., & Murase, K. (1998b). *Analysis of the scenery perceived by a real mobile robot Khepera Lecture Notes in Computer Science*, vol. 1478. Berlin: Springer pp. 295–302.

Oseledec, V. I. (1968). A multiplicative ergodic theorem, Lyapunov characteristic numbers for dynamical systems. *Transactions of the Moscow Mathematical Society*, *19*, 197–231.

Ott, E. (1993). *Chaos in dynamical systems*. Cambridge: Cambridge University Press.

Parker, T. S., & Chua, L. O. (1987). Chaos: A tutorial for engineers. *Proceedings IEEE*, *75*(8), 982–1008.

Pfeiffer, R. (1995). Cognition-perspectives from autonomous agents. *Robotics and Autonomous Systems*, *15*, 47–70.

Pfeiffer, R., & Scheier, C. (1997). Sensory-motor coordination: The metaphor and beyond. *Robotics and Autonomous Systems*, *20*, 157–178.

Sauer, T., Yorke, J. A., Casdagli, M., & Embedology (1991). *Journal Statistical Physics*, *65*, 579–616.

Shimada, I., & Nagashima, T. (1979). A numerical approach to ergodic problem of dissipative dynamical systems. *Progress Theoretical Physics*, *61*(6), 1605–1616.

Smithers, T. (1995). On quantitative performance measures of robot behavior. *Robotics and Autonomous Systems*, *15*, 107–133.

Takens, F. (1981). Detecting strange attractors in turbulence. In D. A. Rand, & L. S. Young, *Lecture notes in mathematics* (Vol. 898) (pp. 366–381). Berlin: Springer, 366–381.

Tani, T. (1996). Model-based learning for mobile robot navigation from the dynamical systems perspective. *IEEE Transactions on System, Man and Cybernetics Part B (Special Issue on Robot Learning)*, *26*, 421–436.

Timmer, J., Haussler, S., Lauk, M., & Lucking, C. H. (2000). Pathological tremors: Deterministic chaos or nonlinear stochastic oscillators? *Chaos*, *10*, 278–288.

Wolf, A., Swift, J. B., Swinney, H. L., & Vastano, J. A. (1985). Determining Lyapunov exponents from a time series. *Physica*, *16D*, 285–317.

Yamaguchi, A., Watanabe, H., Mikami, S., & Wada, M. (1999). Characterization of biological internal dynamics by the synchronization of coupled chaotic system. *Robotics and Autonomous Systems*, *28*, 195–206.

Ziemke, T. (1996a). Towards autonomous robot control via self-adapting recurrent networks. In von der Malsburg, von Seelen, Vorbruggen, & Sendhoff (Eds.), *Artificial neural networks-ICANN'96* (pp. 611–616). Berlin: Springer, 611–616.

Ziemke, T. (1996b). Towards adaptive behavior system integration using connectionist infinite state automata. In P. Maes, M. Mataric, J.-A. Meyer, J. B. Pollack, & S. Wilson (Eds.), *From animals to animats 4: Proceedings of the fourth international conference on simulation of adaptive behavior (SAB'96)* (pp. 145–154). Cambridge, MA: MIT Press, 145–154.

Ziemke, T. (1998) Adaptive behavior in autonomous agents. PRESENCE (Special issue on autonomous agents, adaptive behaviors, and distributed simulations). 796 (pp. 564–587).